Table 2. Micronucleus assay of MWCNT and chrysotile with CHL/IU cells

Concentration (μg/ml)	MN (‰)	Other relevance (‰)			Growth Index (%)
		Bi-N	Multi-N	MP	
MWCNT					
0	8.5	4.5	2.5	14.5	100
0.02	10.5	3.0	2.5	12.5	94
0.078	9.5	6.0	2.5	11.5	88
0.31	12.0	19.0**	5.0	12.0	79
1.3	13.0	27.5**	10.5**	10.0	73
5.0	14.0	63.5**	21.5**	9.5	63
Cochran- Armitage test	$p<0.05$	$p<0.01$	$p<0.01$	–	–
MMC	48.5**	9.5	5.0	9.5	–
Chrysotile					
0	16.0	4.0	2.5	30.0	100
0.1	17.0	4.0	4.5	27.5	98
0.2	22.5	7.5	4.5	25.5	99
0.4	24.0*	40.0**	12.5**	20.5	89
0.8	24.5*	52.5**	14.0**	22.0	86
1.6	30.5**	68.0**	32.5**	23.0	84
Cochran- Armitage test	$p<0.01$	$p<0.01$	$p<0.01$	–	–
MMC	82.0**	5.5	8.5**	21.5	–

Fisher's exact test. * $p<0.05$, ** $p<0.01$. MN: micronucleated cell; Bi-N: bi-nucleated cell; Multi-N: multi-nucleated cell having more than two nuclei; MP: mitotic cell; MMC: Mitomycin C at 0.01 μg/ml. Observed number of cells was 2,000 cells per dose.

polyploidy corresponded to those at which the cell viability, as indicated by the growth index, exceeded 60% for MWCNT and 80% for chrysotile. MMC, which was used as a positive control, did not induce the numerical chromosome aberration but significantly increased the frequency of structural chromosome aberrations which consisted primarily of chromatid break and exchange.

Micronucleus induction

As shown in Table 2, no statistically significant increase in the number of micronucleated cells was found at any dose level of MWCNT as compared with the negative control, although MWCNT exhibited a statistically significant dose-dependent micronucleus induction as indicated by the Cochran-Armitage test. Chrysotile showed a statistically significant increase in the number of micronucleated cells at 0.4 μg/ml and above, in addition to a significant dose-response relationship for the micronucleated cells. However, it should be pointed out that the number of micronucleated cells induced by MWCNT or chrysotile at the maximum dose level increased by less than 2-fold as compared with the respective negative controls. This result indicates that the statistical increase is marginal. On the other hand, MWCNT significantly increased the numbers of bi-nucleated and multi-nucleated cells at 0.31 μg/ml and above and at 1.3 μg/ml and above, respectively, as compared with the negative controls, and also in a dose-dependent manner as indicated by the Cochran-Armitage test. Notably, the numbers of bi-nucleated and multi-nucleated cells induced by MWCNT at 5.0 μg/ml were increased 14- and 8.6-fold, respectively, as compared with the respective control levels. Chrysotile also significantly increased the bi-nucleated and multi-nucleated cells at 0.4 μg/ml and above in a dose-dependent manner. Statistically significant induction of bi-nucleated cells by chrysotile occurred at approximately the same dose level as that by MWCNT on an equal mass basis. The numbers of bi-nucleated and multi-nucleated cells induced by chrysotile at 1.6 μg/ml were increased 17- and 13-fold, respectively, as compared with the respective control levels. The minimum dose levels of MWCNT and chrysotile for the significant induction of bi-nucleated and multi-nucleated cells corresponded to those at which the cell viability as indicated by the growth index exceeded 70% for MWCNT and 80% for chrysotile. MMC markedly induced micronuclei without the formation of bi-nucleated cells.

Mutation at the hgprt locus

Table 3 shows mutation rates and viabilities of CHL/IU cells exposed to MWCNT or chrysotile at different

Table 3. Mutagenicity of MWCNT and chrysotile at the *hgprt* locus with CHL/IU cells

Concentration (μg/ml)	Viability(%)	Mutation rate per 10^6 cells
MWCNT		
0	100	4.68
6.3	86	3.56
12.5	63	6.83
25	48	4.77
50	33	6.14
100	21	3.82
EMS	33	462*
Chrysotile		
0	100	5.53
1.56	73	7.38
3.13	54	6.63
6.25	43	5.33
12.5	23	2.32
25	17	1.53
EMS	48	325*

EMS: ethyl methanesulfonate at 200 μg/ml. *: Positive response.

dose levels. Neither MWCNT nor chrysotile was negative for the mutagenicity at the *hgprt* locus with CHL/IU cells, although the exposures to MWCT and chrysotile decreased the cell viabilities to 21% and 17%, respectively, in a dose-dependent manner. Exposure of CHL/IU cells to EMS, a positive control, at 200 μg/ml induced clearly positive mutagenicity at the *hgprt* locus.

Cellular uptake of MWCNT and chrysotile

Light-microscopic observation, shown in Fig. 3A, revealed that dispersed and isolated MWCNT fibers were internalized in CHL/IU cells and were localized in the cytoplasm. Long MWCNT fiber bridging two cells and a multi-nucleated cell noteworthy. Cellular internalization of MWCNT was confirmed by SEM observation, as shown in Fig. 3B. The cellular uptake of MWCNT fibers was incomplete, and Fig. 3B shows a MWCNT fiber of longer than 5 μm penetrating into a cell in the highly magnified inset. Both phase-contrast microscopic and SEM observations also showed cellular uptake and localization of long chrysotile (Fig. 3C), and incomplete internalization and cytoplasmic penetration of chrysotile fibers longer than 10 μm (Fig. 3D) in the same manner as MWCNT.

Discussion

Cytotoxicity

In the present study, MWCNT-exposed CHL/IU cells exhibited a dose-dependent increase in cytotoxicity as evaluated by both the colony formation and LDH assays. The degree of MWCNT-induced cytotoxicity was found to depend on the solvent used for suspension of hydrophobic MWCNT and the ultrasonication duration of the MWCNT suspension. Suspension of MWCNT in DMSO/culture medium and subsequent 3-minute ultrasonication induced the highest MWCNT-induced cytotoxicity, giving the most sensitive dose-response relationship of cytotoxicity as evaluated by the colony formation assay. It was also found by DLS measurement that the hydrodynamic diameter of MWCNT decreased in the following order of solvents: Tween 80>CMC>culture medium>DMSO/ culture medium under a fixed condition of 3-minute ultrasonication ; and hydrodynamic diameters decreased in the following order of ultrasonication duration: 1 min>3 min=10 min in the of DMSO/culture medium. Therefore, it can be inferred from the present results that the degree of MWCNT-induced cytotoxicity tended to increase with a decrease in the hydrodynamic diameter of MWCNT in the culture medium, presumably due to the effective dispersion of agglomerated MWCNT to isolated MWCNT by ultrasonication and also the solvent, containing DMSO and serum. DMSO has been reported to facilitate good dispersion of hydrophobic MWCNT[11] at 0.5% which is below the DMSO concentration that inhibited cellular death due to scavenging reactive oxygen species (ROS) at concentrations ranging from 140 to 280 mM[29]. Consistently, our SEM observation confirmed good dispersion of agglomerated MWCNT into single, isolated fibers in the DMSO/culture medium after the 3-minute ultrasonication (Fig. 1C). However, it should be pointed out that although the 10-minute ultrasonication produced

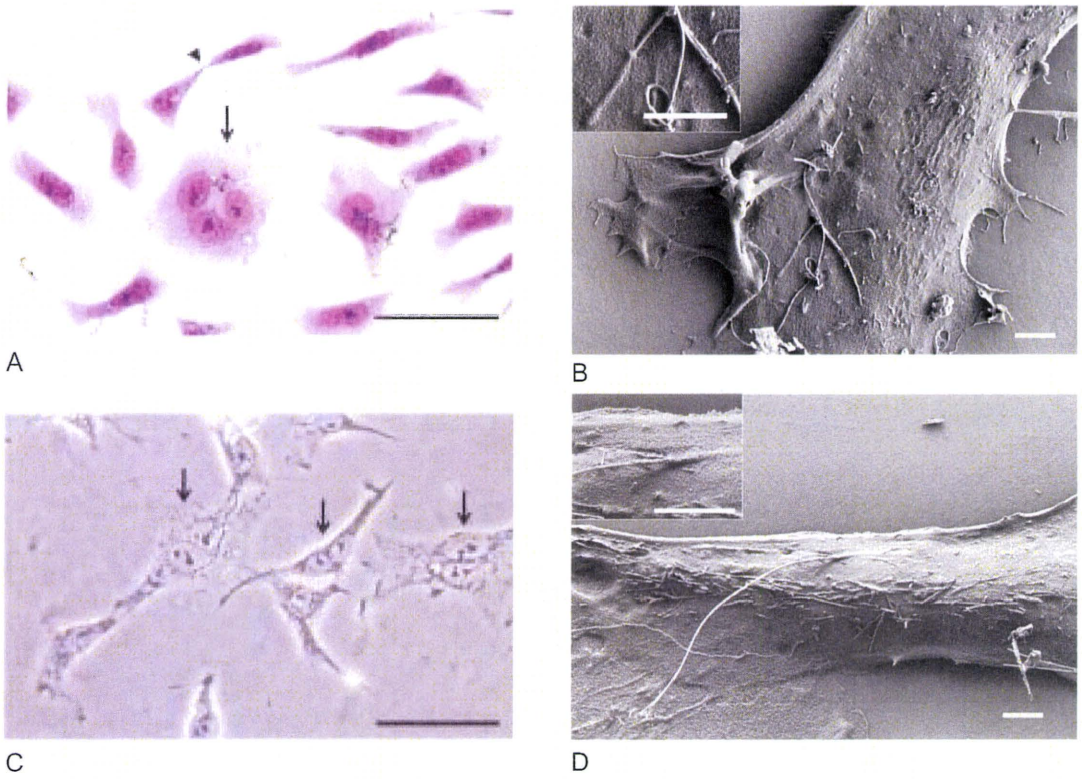

Fig. 3. CHL/IU cells exposed to MWCNT (A and B) or chrysotile (C and D). A: Light-microscopic image of the CHL/IU cells exposed to MWCNT at 4.0 μg/m*l* for 48 h. A multi-nucleated cell is observed in the center (arrow), and a 20-μm long MWCNT fiber on the upper side (arrowhead) bridges two cells. Bar indicates 50 μm ; Giemsa stain. B: A SEM image showing single, isolated MWCNT fibers incompletely internalized into a cell. The inset is a higher magnification of the same cell to show the MWCNT fiber penetrating into the cell. Bars indicate 2 μm. C: Phase-contrast microscopic image of cells exposed to chrysotile at 5.0 μg/m*l* for 48 h. Several bi-nucleated CHL/IU cells are observed (arrows). Chrysotile fibers are localized in the cytoplasm. No staining ; Bar indicates 50 μm. D: A SEM image showing a single chrysotile fiber incompletely internalized into a CHL/IU cell. The inset is a higher magnification of the same cell showing the chrysotile fiber penetrating beneath the surface of the cell membrane. Bars indicate 2 μm.

a submicron-sized, small peak of 300 nm in hydrodynamic diameter, the cytotoxicity of MWCNT after the 10-minute ultrasonication was less potent than that after the 3-minute ultrasonication. This result suggests that exposure of CHL/IU cells to the submicron-sized MWCNT at the relatively low levels does not enhance the cytotoxicity.

The present result that MWCNT induced dose-dependent release of LDH from CHL/IU cells is comparable with the finding of Muller *et al.*[8] that MWCNT induced a dose-dependent increase in the release of LDH from rat lung epithelial (RLE) cells together with decreased mitochondrial activity in the same cells as measured with the dimethylthiazole-tetrazolium (MTT) assay. It has been generally recognized that cytotoxicity is causally related to cellular internalization of CNT[30], while cellular generation of ROS is involved in the mechanism of cytotoxicity for asbestos fibers[31], in addition to internalization. However, it remains unclear whether the internalized CNT causes cytotoxicity through generation of ROS. Unpurified, iron-rich CNT but not purified CNT was reported to produce ROS in *in vitro* studies[18–20]. Recently, Tabet *et al.*[13] reported that MWCNT containing 2% iron decreased *in vitro* cell viability without internalization of MWCNT in human lung epithelial cells or production of intracellular oxidative responses as implied by RNA expression of different genes. It is noteworthy in the present study that both MWCNT and chrysotile were incompletely internalized in CHL/IU cells, resulting in cytoplasmic penetration of these two fibers, and localization in the cytoplasm (Fig. 3). Consistent with the present observation, cellular uptake of MWCNT has been demonstrated by light- and electron-microscopy[9, 10, 14, 18, 21]. In this context, it is also interesting to note that *in vivo* exposure to long and thin MWCNT fibers caused frustrated phagocytosis and multi-nucleated

giant cells as reported by Poland *et al.*[6] and incomplete cytoplasmic penetration of fibers as reported by Hubbs *et al.*[32]. Therefore, MWCNT-induced cytotoxicity might be causally related to possible isolation and dispersion of agglomerated MWCNT in the DMSO/culture medium, which would facilitate uptake of MWCNT fibers into CHL/IU cells, possibly causing cellular impairment by the MWCNT fibers, and leading to growth inhibition and cellular death. Our previous study[26] suggested, on the basis of Fe analysis and two *in vitro* and *in vivo* findings[18, 19], that an iron content of 0.44% in MWCNT exerts little effect on cell viability through Fe-induced ROS production, since pharyngeal aspiration of purified SWCNT containing 0.23% Fe in mice did not generate detectable signals from iron paramagnetic centers that would be readily detectable by ESR spectroscopy in the unrefined, iron-rich SWCNT[18]. Also, iron-rich SWCNT (26% Fe) caused significant loss of intracellular GSH and accumulation of lipid hydroxides in RAW 264.7 macrophages as compared with iron-stripped SWCNT (0.23% Fe)[19]. In this context, it was noteworthy in the present study that the cytotoxicity of chrysotile was more potent than that of MWCNT on an equal mass basis, although there are similarities in iron content and size distribution between MWCNT and chrysotile fibers[25–27]. The surface properties of MWCNT as well as its physical dimension may play important roles in its cytotoxicity, as suggested by Tian *et al.*[16].

Genotoxicity

The *in vitro* genotoxicity of MWCNT found in the present study can be characterized by numerical but not structural chromosome aberration. Chromosomes showed polyploidy, and significantly increased numbers of bi-nucleated and multi-nucleated cells without clear micronucleus induction, as well as negative *hgprt* mutagenicity. Chrysotile exhibited genotoxicity which was essentially the same as MWCNT, except for marginal but significant induction of micronuclei.

It has been reported that MWCNT shows negative bacterial mutagenicity in the presence and absence of metabolic activation[22–24]. The present *hgprt* mutagenicity assay can detect gene mutation in mammalian cells and confirmed the negative mutagenicity of MWCNT and chrysotile for CHL/IU cells as demonstrated by the bacterial mutagenicity assay. It is indicated, therefore, that neither MWCNT nor chrysotile interact directly with DNA.

The present results for MWCNT in the chromosome aberration assay can be contrasted with the findings of Muller *et al.*[8] that MWCNT statistically increased the numbers of bi-nucleated MCF-7 cells containing centromere-positive and -negative micronuclei, and that the frequency of micronucleated cells of both RLE and human breast carcinoma (MCF-7) exposed to MWCNT was increased in a dose-dependent manner. Their former finding with the fluorescence *in situ* hybridization (FISH) using a human pancentromeric probe is considered to be suggestive of the occurrence of both clastogenic and aneugenic events induced by MWCNT. However, the present results from the chromosome aberration and micronucleus induction assays revealed that MWCNT induces polyploidy but not micronuclei in a manner similar to chrysotile, while both MWCNT and chrysotile significantly increased the numbers of bi-nucleated and multi-nucleated cells. Since the distribution of lengths of MWCNT fibers was skewed to longer lengths than that for chrysotile, and since the long fibers of MWCNT were similar in appearance to those of asbestos fibers[6, 25–27], the mechanisms underlying significant induction of bi-nucleated and multi-nucleated cells by MWCNT can be surmised on the basis of the following literature. Jensen *et al.*[33] demonstrated that long crocidolite asbestos fibers cause polyploidy by sterical blocking of cytokinesis, leading to the formation of bi-nucleated cells. Shi and King[34] reported that chromosome non-disjunction is tightly coupled to cytokinesis failure resulting in the formation of tetraploid cells, and that coupling of chromosome non-disjunction with cytokinesis failure may potentiate mis-segregation during subsequent cell division, leading ultimately to the formation of aneuploid cells through multipolar mitosis of tetraploid cells. Taking these findings together, the significant induction of polyploidy without clear micronucleus induction by MWCNT, through the formation of bi-nucleated and multi-nucleated cells, is considered to result from the interference of long and thin MWCNT and chrysotile fibers with components of the mitotic spindle during chromosome segregation or from sterical blocking of cytokinesis. Our inference is consistent with the microscopic observation of Mangum *et al.*[35] that a small fraction of alveolar macrophages from the lung of SWCNT-exposed rats was bridged by intracellular SWCNT that extended into the cytoplasm of two macrophages. It can be suggested, therefore, that the genotoxicity of long and thin MWCNT might be causally related to indirect interactions of MWCNT with DNA causing genomic instability such as aneugenic events, rather than direct interactions of MWCNT with DNA causing mutation and clastogenic events, neither of which were observed in the present study. Long MWCNT fibers have been reported to cause mesotheliomas in mice[4] and rats[5] and to behave like long asbestos fibers in the mouse peritoneal cavity[6]. However, Muller *et al.*[36] reported no significant induction of mesotheliomas in a 2-year bioassay in the peritoneal cavity of rats that received a single intraperitoneal injection of MWCNT, whereas crocidolite induced mesothelioma. Since the MWCNT that Muller *et al.* used was reported to contain short and tangled fibers of about 0.7 μm in length[36], it can be

suggested that long (>5 μm) and straight MWCNT fibers elicit the carcinogenic response. Further study is urgently needed to explore possible causative factors such as physical and physicochemical properties of MWCNT, using in vitro assay systems, such as a cell transformation assay that might reflect the initiation and promotion stages of early carcinogenesis by MWCNT better than the genotoxicity assays used in the present study.

Conclusions

Cytotoxicity of MWCNT depended on the solvent used for suspension of MWCNT and the ultrasonication duration of the suspension, suggesting that the cytotoxicity is causally related to dispersion and isolation of agglomerated MWCNT. The cytotoxicity of chrysotile was greater than that of MWCNT. The genotoxicity of MWCNT and chrysotile was characterized by negative *hgprt* mutagenicity, insignificant induction of micronuclei, the formation of polyploidy without structural chromosome aberration, and increased numbers of bi-nucleated and multi-nucleated cells. SEM observation showed that MWCNT and chrysotile were incompletely internalized in the cells and localized in the cytoplasm. It was suggested that the genotoxicity of MWCNT and chrysotile may arise not from direct interaction with DNA, but from the physical interference of these two fibers with biological processes during cytokinesis.

Acknowledgment: The present study was supported in part by a Grant-in-Aid for Scientific Research from the Ministry of Health, Labour and Welfare of Japan.

References

1) Martin CR, Kohli P. The emerging field of nanotube biotechnology. Nat Rev Drug Discov 2003; 2: 29–37.
2) Toray Corporate Business Research, INC. Report on the survey of production and use of nanomaterials in Japan, -Fy 2008- (in Japanese).
3) Han JH, Lee EJ, Lee JH, et al. Monitoring multiwalled carbon nanotube exposure in carbon nanotube research facility. Inhal Toxicol 2008; 20: 741–9.
4) Takagi A, Hirose A, Nishimura T, et al. Induction of mesothelioma in p53+/– mouse by intraperitoneal application of multi-wall carbon nanotube. J Toxicol Sci 2008; 33: 105–16.
5) Sakamoto Y, Nakae D, Fukumori N, et al. Induction of mesothelioma by a single intrascrotal administration of multi-wall carbon nanotube in intact male Fischer 344 rats. J Toxicol Sci 2009; 34: 65–76.
6) Poland CA, Duffin R, Kinloch I, et al. Carbon nanotubes introduced into the abdominal cavity of mice show asbestos-like pathogenicity in a pilot study. Nature Nanotechnol 2008; 3: 423–8.
7) Shvedova AA, Kisin E, Murray AR, et al. Inhalation vs. aspiration of single-walled carbon nanotubes in C57BL/6 mice: inflammation, fibrosis, oxidative stress, and mutagenesis. Am J Pysiol Lung Cell Mol Physiol 2008; 295: 552–65.
8) Muller J, Decordier I, Hoet PH, et al. Clastogenic and aneugenic effects of multi-wall carbon nanotubes in epithelial cells. Carcinogenesis 2008; 29: 427–34.
9) Monteiro-Riviere NA, Nemanich RJ, Inman AO, Wang YY, Riviere JE. Multi-walled carbon nanotube interaction with human epidermal keratinocytes. Toxicol Lett 2005; 155: 377–84.
10) Sato Y, Yokoyama A, Shibata K, et al. Influence of length on cytotoxicity of multi-walled carbon nanotubes against human acute monocytic lelukemia cell line THP-1 in vitro and subcutaneous tissue of rats in vivo. Mol Biosyst 2005; 1: 176–82.
11) Soto K, Garza KM, Murr LE. Cytotoxic effects of aggregated nanomaterials. Acta Biomater 2007; 3: 351–8.
12) Hirano S, Kanno S, Furuyama A. Multi-walled carbon nanotubes injure the plasma membrane of macrophages. Toxicol Appl Pharmacol 2008; 232: 244–51.
13) Tabet L, Bussy C, Amara N, et al. Adverse effects of industrial multiwalled carbon nanotubes on human pulmonary cells. J Toxicol Environ Health, Part A 2009; 72: 60–73.
14) Simon-Deckers A, Gouget B, Mayne-L'hermite M, Herlin-Boime N, Reynaud C, Carriere RM. In vitro investigation of oxide nanoparticle and carbon nanotube toxicity and intracellular accumulation in A549 human pneumocytes. Toxicology 2008; 253: 137–46.
15) Manna SK, Sarkar S, Barr J, et al. Single-walled carbon nanotube induces oxidative stress and activates nuclear transcription factor -kappaB in human keratinocytes. Nano Lett 2005; 5: 1676–84.
16) Tian F, Cui D, Schwarz H, Estrada GG, Kobayashi H. Cytotoxicity of single-wall carbon nanotubes on human fibroblasts. Toxicol In Vitro 2006; 20: 1202–12.
17) Jacobsen NR, Pajana G, White P, et al. Genotoxicity, cytotoxicity, and reactive oxygen species induced by single-walled carbon nanotubes and C (60) fullerenes in the FEl-Mutatrade markMouse lung epithelial cells. Environ Mol Mutagen 2008; 49: 476–87.
18) Pulskamp K, Diabate S, Krug HF. Carbon nanotubes show no sign of acute toxicity but induce intracellular reactive oxygen species in dependence on contaminants. Toxicol Lett 2007; 168: 58–74.
19) Shvedova AA, Castranova V, Kisin ER, et al. Exposure to carbon nanotube material: assessment of nanotube cytotoxicity using human keratinocyte cells. J Toxicol Environ Health, Part A 2003; 66: 1909–26.
20) Kagan VE, Tyurina YY, Tyurin VA, et al. Direct and indirect effects of single walled carbon nanotubes on RAW 264.7 macrophages: role of iron. Toxicol Lett 2006; 165: 88–100.
21) Zhu L,Chang DW, Dai L, Hong Y. DNA damage induced by multiwalled carbon nanotubes in mouse embryonic stem cells. Nano Lett 2007; 7: 3592–7.
22) Miyawaki J, Yudasaka M, Azami T, Kubo Y, Iijima S. Toxicity of single-walled carbon nanohorns. ACS Nano

2000; 2: 213–26.
23) Di Sotto A, Chiaretti M, Carru GA, Belluci S, Mazzanti G. Multi-walled carbon nanotubes: lack of mutagenic activity in the bacterial reverse mutation assay. Toxicol Lett 2009; 184: 192–7.
24) Wirnitzer U, Herbold B, Voetz M, Ragot J. Studies on the in vitro genotoxicity of baytubes, agglomerates of engineered multi-walled carbon-nanotubes (MWCNT). Toxicol Lett 2009; 186: 160–5.
25) Murr LE, Soto KF. TEM comparison of chrysotile (asbestos) nanotube and carbon nanotubes. J Mater Sci Lett 2004; 39: 4941–7.
26) Takaya M, Serita F, Yamazaki K, et al. Characteristics of multiwall carbon nanotubes for an intratracheal instillation study with rats. Ind Health 48 (In press).
27) Langer AM, Nolan RP. Chrysotile: its occurrence and properties as variables controlling biological effects. Ann Occup Hyg 1994; 38: 427–51.
28) Ishidate M Jr., Odashima S. Chromosome tests with 134 compounds on Chinese hamster cells in vitro—a screening for chemical carcinogens. Mutat Res 1977; 48: 337–54.
29) Pourahmad J, O'Brien PJ. A comparison of hepatocyte cytotoxic mechanisms for Cu^{2+} and Cd^{2+}. Toxicology 2000; 143: 263–73.
30) Jaurand MC, Renier A, Daubriac J. Mesothelioma: do asbestos and carbon naotubes pose the same health risk? Particle and Fibre Toxicol 2009: 6: 1–16.
31) Manning CB, Vallyathan V, Mossman BT. Diseases caused by asbestos: mechanisms of injury and disease development. Int Immunopharmacol 2002; 2: 191–200.
32) Hubbs A, Mercer RR, Coad JE, et al. Persistent pulmonary inflammation, airway mucous metaplasia and migration of multiwalled carbon nanotubes from the lung after subchronic exposure. The Toxicologist 2009; 108: 457.
33) Jensen CG, Jensen LC, Rieder CL, Cole RW, Ault JG. Long crocidolite asbestos fibers cause polyploidy by sterically blocking cytokinesis. Carcinogenesis 1996; 17: 2013–21.
34) Shi Q, King RW. Chromosome nondisjunction yields tetraploid rather than aneuploid cells in human cell lines. Nature 2005: 437: 1038–42.
35) Mangum JB, Turpin EA, Antao-Menezes A, Cesta MF, Bermudez E, Bonnerr JC. Single-walled carbon nanotube (SWCNT)—induced interstitial fibrosis in the lungs of rats is associated with increased levels of PDGF mRNA and the formation of unique intercellular carbon structures that bridge alveolar macrophages in situ. Particle Fibre Toxicol 2006; 3: 315–28.
36) Muller J, Delos M, Panin N, Rabolli V, Huaux F, Lison D. Absence of carcinogenic response to multiwall carbon nanotubes in a 2-year bioassay in the peritoneal cavity of the rat. Toxicol Sci 2009; 110: 442–8.

Industrial Health 2010, 48, 452–459

Original Article

Characteristics of Multiwall Carbon Nanotubes for an Intratracheal Instillation Study with Rats

Mitsutoshi TAKAYA[1]*, Fumio SERITA[1], Kazunori YAMAZAKI[2], Shigetoshi AISO[2], Hisayo KUBOTA[1], Masumi ASAKURA[2], Naoki IKAWA[2], Kasuke NAGANO[2], Heihachiro ARITO[2] and Shoji FUKUSHIMA[2]

[1]National Institute of Occupational Safety and Health, 6–21–1 Nagao, Tama-ku, Kawasaki, Kanagawa, 214-8585, Japan

[2]Japan Bioassay Research Center, Japan Industrial Safety and Health Association, 2445 Hirasawa, Hadano, Kanagawa, 257-0015, Japan

Received July 23, 2009 and accepted December 3, 2009

Abstract: Much concern has been raised over the health consequences of workers exposed to carbon nanotubes. In order to characterize multi-wall carbon nanotubes (MWCNT) suspended in a phosphate-buffered saline containing 0.1% Tween 80 for an intratracheal instillation study. Length and width distributions of the MWCNT fibers, dispersion of MWCNT in the suspension and in the lung tissue and the MWCNT contents of metal impurities were investigated. Arithmetic mean length and width of the MWCNT fibers as measured on scanning electron microscope (SEM) photographs were 5.0 μm and 88 nm, respectively, and fibers longer than 5.0 μm were 38.9% of all fibers measured. Dynamic light scattering size measurement revealed that 5-min ultrasonication, together with addition of Tween 80 into the suspension, decreased the hydrodynamic diameters of the agglomerated MWCNT to those of finer particles below 1.0 μm. SEM observation showed good dispersion of MWCNT in the suspension, and in the alveoli on Day 1 after instillation. Concentration of iron, chromium and nickel in the MWCNT were 4,400, 48 and 17 ppm (wt/wt), respectively, all of which were below levels that would elicit positive pulmonary toxic responses to these metals. The results suggest that well-dispersed, long and thin MWCNT fibers exhibit asbestos-like pathogenicity in the lung.

Key words: Multiwall carbon nanotube, Metal impurities, Iron, SEM, Dynamic light scattering, Size distribution, Dose characterization

Introduction

In this decade, one of the most important developed in industrial technology is nanotechnology which makes use of nano-scale (<100 nm) structure-controlled materials. Use of nanotechnology is expected to grow exponentially in the first half of the 21st century. The growth of nanotechnology industries has prompted a rapid increase in amounts and kinds of nanomaterial production. However, the increased use of nanomaterials may result in new types of health risks for workers exposed to nanomaterials.

*To whom correspondence should be addressed.
E-mail: takaya@h.jniosh.go.jp

At present, health hazards of nanomaterials have not been clarified sufficiently yet, and many researchers have been extensively investigating biological responses to nanomaterials, using *in vivo* and *in vitro* techniques. Among the many types of nanomaterials, carbon nanotubes (CNT) have raised much attention and concern, since their fibrous forms are similar to those of asbestos. Recent studies by Takagi *et al.*[1)] and Sakamoto *et al.*[2)] showed that mesotheliomas are induced by intraperitoneal and intrascrotal administrations of multiwall carbon nanotubes (MWCNT) in p53 gene-deficient mice and male Fischer 344 rats, respectively. Poland *et al.*[3)] also demonstrated the asbestos-like pathogenicity of long MWCNT fibers administered to the peritoneal cavity of female mice. Since inhalation is the primary

route of exposure of workers to carbon nanotubes, and since the target organ is the respiratory system, use of an inhalation exposure system would be recommended for a study of experimental toxicology. Because of the technical difficulty in generating stable MWCNT aerosol at a constant concentration for an inhalation study, the technique of intratracheal instillation or pharyngeal aspiration has been extensively used to examine the pulmonary toxicity of nanomaterials in spite of the limitations of intratracheal instillation[4]. Since MWCNT is agglomerated in a rope-like structure and insoluble in aqueous solutions, use of well-dispersed MWCNT fibers suspended in an aqueous solution containing a dispersant is a prerequisite in an intratracheal instillation study evaluating the pulmonary toxicity of MWCNT. Indeed, Mercer *et al.*[5] reported that exposure of mice to well-dispersed single-wall carbon nanotubes (SWCNT) fibers by pharyngeal aspiration affected pulmonary distribution and responses. It has also been reported that in addition to the size, shape and agglomerated state[3, 6], the content of iron used for catalysis[7–9] modified the pulmonary responses of rats and mice to CNT.

In order to evaluate the pulmonary responses of rats to MWCNT by administered intratracheal instillation, information about the characteristics of MWCNT such as length and width of MWCNT fibers, dispersion of MWCNT in the suspension and in the lung tissue and metal impurities in MWCNT is of prime importance. Therefore, the present study measured the length and width of dispersed MWCNT fibers in a suspension by scanning electron microscopic (SEM) observation, to explore how to well-disperse MWCNT fibers in a suspension and in lung tissues, and to determine concentrations of metal impurities in MWCNT that might modify the pulmonary responses to MWCNT. The results of the pulmonary toxic responses of male Fischer 344 rats to the intratracheally instilled MWCNT under the same conditions of dosage as those obtained in the present study were submitted to Industrial Health as a separate paper[10].

Materials and Methods

Test substance

MWCNT used in the present study was kindly supplied by Mitsui & Co., Ltd. (MWCNT-7, Lot No. 061220, Tokyo, Japan). This MWCNT was synthesized by the vapor phase chemical vapor deposition (CVD) and graphitization following CVD. Most manufacturers with large-scale production of MWCNT have adopted vapor phase CVD according to their published information[11, 12]. The MWCNT used in the present study was a typical sample of MWCNT being manufactured at present.

Size distribution and dispersion of MWCNT in the suspension

MWCNT was suspended in phosphate-buffered saline (PBS) containing 0.1% Tween 80 as a dispersant. Then, the suspension was subjected to ultrasonication with an ultrasonic homogenizer (VP-30S, 20 kHz, 300 W, TAITEC Co., Ltd, Tokyo, Japan) for various periods of time.

The size distribution of MWCNT in the suspension was evaluated by both SEM observation and dynamic light scattering size (DLS) measurement. Sample preparation for SEM observation of fibers was described in detail in our previous paper[13]. Briefly, a water drop of MWCNT suspension at 533 μg/ml was put on a polycarbonate membrane filter (Isopore, Millipore, MA, USA) set on a suction filtration apparatus. A drop of the sample suspension was put onto another pre-settled water-drop, and the suction was started. The filtered membrane filter samples were dried in air. After drying the filter was pre-coated with Pt-Pd for electron charge avoidance, and the MWCNT fibers were observed with a field emission SEM (S-4700, Hitachi, Tokyo, Japan). Several fields of viewing were photographed at magnifications of × 1,000 and × 5,000 for measurement of length and width, respectively. The length and width of MWCNT fibers, almost all of which appeared to be isolatably thin in each field, were measured with a curvimeter and scale loupe on enlarged photoprints. The number of fibers used in the length and width measurements were 1,000 and 500, respectively. The DLS measurement with a Zetasizer Nano DLS analyzer (Malvern, Worcestershire, UK) was performed on the PBS-Tween 80 suspension containing MWCNT at 533 μg/ml. In order to prevent excessive lung burden of MWCNT, we chose the level of 533 μg/ml which is equivalent to an intratracheally instilled dose of 160 μg/rat, based on Morrow's report[14] that the level of dust burden causing lung overload was greater than 1–2 mg of persistently retained dust in the lungs of F344 rats.

Dispersion of MWCNT in the aerosolized suspension and in the lung

In order to observe the dispersed state of MWCNT fibers in the PBS-Tween 80 suspension exactly at the time of intratracheal instillation, the suspension containing MWCNT at 533 μg/ml was ejected into the air from the tip of the microspray cannula of an Intratracheal Aerosolizer (1A-1B, PennCentury, Inc., USA) which was connected to a syringe pre-filled with the MWCNT suspension. The experimental set-up for aerosolization in a glove-box is presented in Fig. 1. The aerosol-

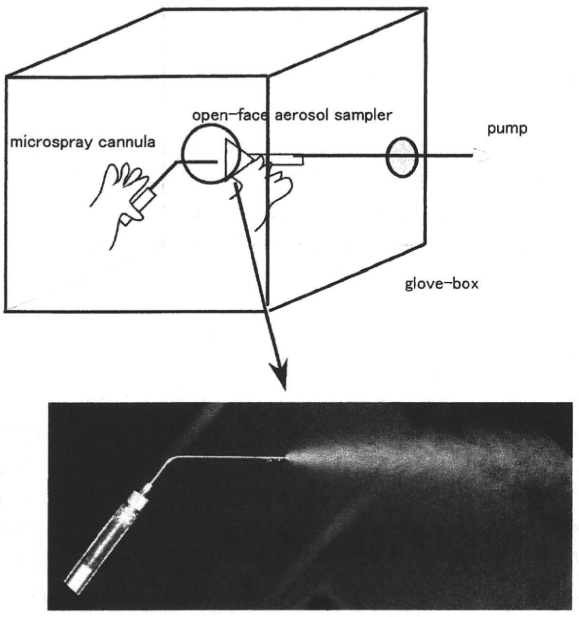

Fig. 1. The experimental set-up was installed in a glove-box (A). Aerosolized MWCNT suspension was ejected into the air from the tip of a microspray cannula which was connected with a syringe filled with the MWCNT suspension (B). The concentration of MWCNT suspension used was 533 μg/ml (equivalent to a dose of 160 μg in 0.3 ml suspension).

ized MWCNT suspension was collected on a 25-mm Isopore-membrane filter using an open-face aerosol sampler which was connected to a sampling pump (Lelandpump, SKC, USA). The sampling rate was 9 l/min, and the distance between the filter sampler and the tip of the microspray cannula was about 20 cm. The filter sample was dried in air, and after drying the filter was pre-coated with Pt-Pd. The sample was observed with the SEM.

In order to examine whether the well-dispersed state of the MWCNT fibers after intratracheal instillation was maintained in the lung tissues, the deposition of MWCNT in left lung tissues of the rats which received intratracheal instillation at a dose of 160 μg/rat was examined by SEM one day 1 after instillation[10].

Analysis of metal impurities in MWCNT

At first, the MWCNT was analyzed qualitatively for metals by Laser-Abrasion Inductively Coupled Mass Spectrometry (LA-ICP-MS). Figure 2 shows the procedure of sample preparation for LA-ICP-MS analysis. MWCNT was suspended in ethanol, and a portion of the suspension was put onto a PTFE membrane filter (Omnipore, Millipore, Billerica, MA, USA). The filter sample was fixed to a slide glass (Matsunami Glass Industry, Kishiwada, Japan) using ultraviolet curing glue (Three Bond 1771E, Three bond, Hachioji, Japan), and then pressed with 500 g weight. The fixed particle samples were vaporized by a 213 nm NdYAG laser (UP-213 Electro Scientific Industry, Portland, OR, USA) and the vapor was introduced into an Inductively Coupled Plasma-Mass Spectrometer (Agilent 7500c, Yokogawa Analytical, Tokyo, Japan) for qualitative analysis of the elements.

After the qualitative analysis, the detected metal impurities were analyzed quantitatively by graphite furnace atomic absorption spectrometry (AAS) as follows. About 20 mg of MWCNT was weighed, then the sample was digested with 5 ml of hydrochloric acid, 2.5 ml of nitric acid and 5 ml water solution for 30 min heating at 160°C. After cooling, the solution was diluted by 0.5% nitric acid to 50 ml. The metal concentrations in the sample solution were measured by a graphite atomic absorption spectrometer (Z-5010, Hitachi, Tokyo, Japan).

Results

Length and width of MWCNT fiber

Figure 3 shows the distribution of lengths and widths of MWCNT fibers as determined by the SEM analysis. The arithmetic mean and SD of the fiber lengths were 5.0 ± 4.5 μm, ranging from 0.5 μm at the minimum to 21.8 μm at the maximum. The fibers with lengths greater than 5 μm were 38.9% of fibers measured, indicating that the distributions of the lengths was skewed with longer fibers. The arithmetic mean and SD of the fiber width were 88 ± 5 nm, ranging from 40 nm at the minimum to 173 nm at the maximum.

Dispersion of MWCNT fibers in the suspension and in the lung tissue

In order to facilitate dispersion of the MWCNT fibers, Tween 80 was added at a concentration of 0.1% in the suspension in the present study. Figure 4 shows the effect of ultrasonication on MWCNT particle sizes evaluated by the DLS measurement for the hydrodynamic diameter which was numerically derived from optical measurement of the Brownian motion of the target particles, on the assumption that the particles were spherical. Five minutes ultrasonication of the MWCNT suspension was found to completely eliminate the second peak with a diameter of 7.0 μm, decrease the diameter of the main peak from 2.0 μm to below 1.0 μm, and create a new fraction of MWCNT of 0.2 μm in diameter. A SEM image indicating good dispersion of the MWCNT fibers in the suspension is presented in Fig. 5A. In the simulation experiment (Fig. 1), the microspray cannula was found to completely aerosolize

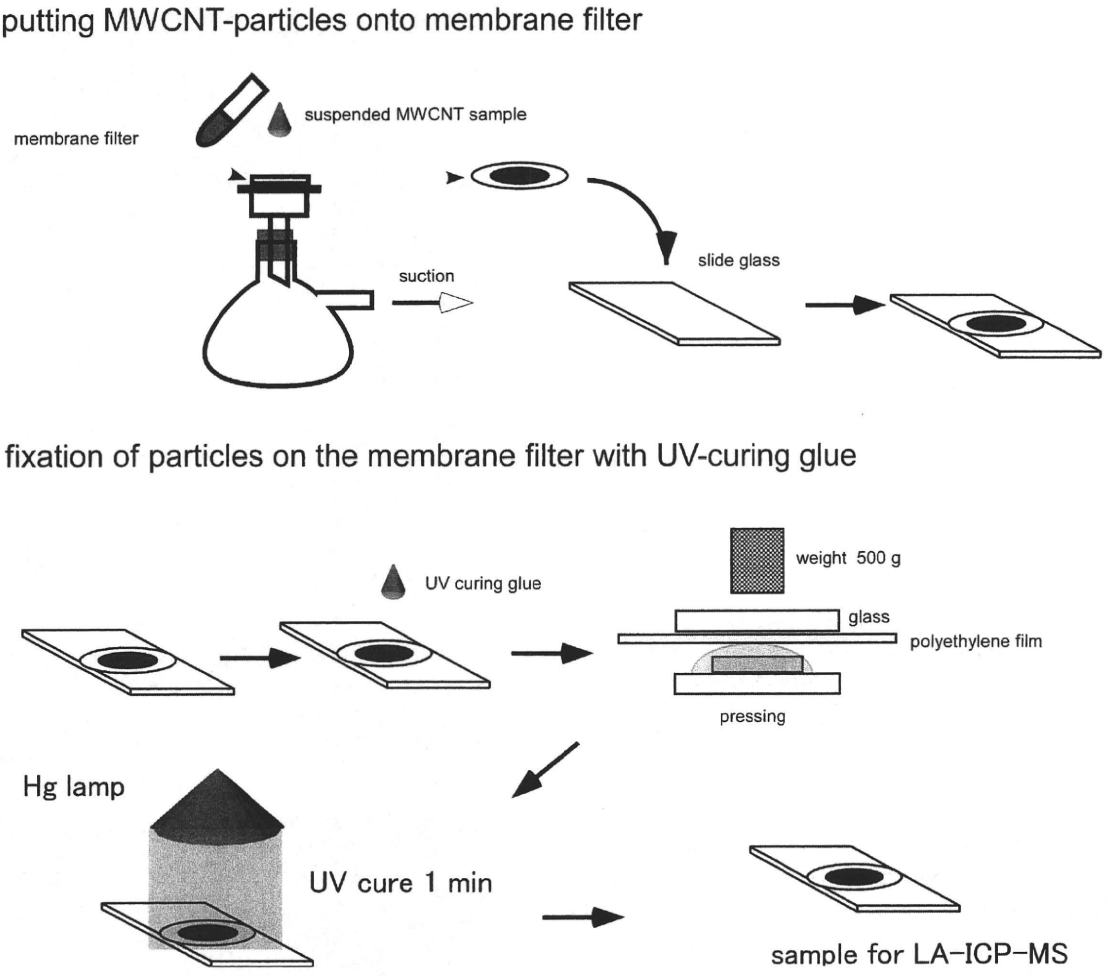

Fig. 2. A schematic diagram of the procedure of the sample preparation for the LA-ICP-MS analysis.

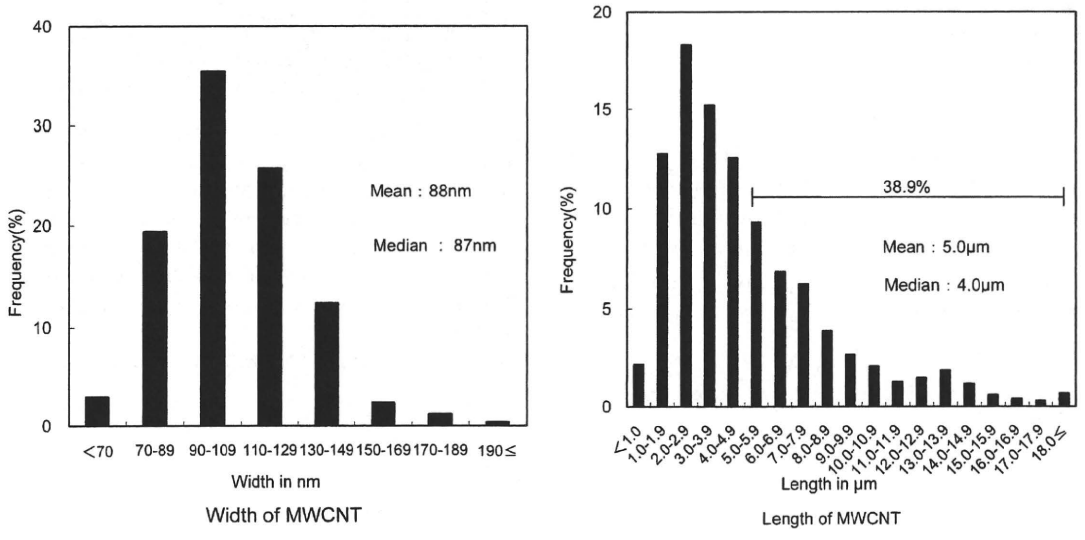

Fig. 3. Histograms of length (A) and width (B) of MWCNT fibers as measured with a curvimeter and a scale loupe, respectively, on the enlarged photographs of SEM image.

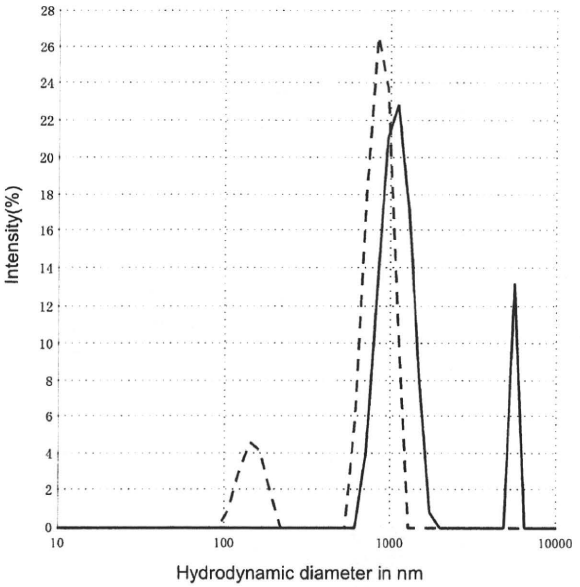

Fig. 4. Effect of ultrasonication on dispersion of MWCNT in the PBS suspension in the presence of 0.1% Tween 80 as a dispersant.
The concentration of MWCNT in the suspension was fixed at 533 μg/ml. The solid line indicates the suspension without ultrasonication, while the dashed line represents the sample ultrasonicated for 5 min.

the MWCNT suspension without forming droplets at the tip. Figure 5B shows that the well-dispersed state of MWCNT fibers was maintained at the time of intratracheal instillation in the same manner as in the suspension before the instillation. A SEM image (Fig. 5C) reveals that MWCNT fibers were well-dispersed in the alveoli on Day 1 after instillation, and that the dispersed fibers appear to be penetrated from the cytoplasm of alveolar macrophages after phagocytosis or incomplete phagocytosis.

Metal impurities in the MWCNT

The qualitative analysis by LA-ICP-MS revealed that the MWCNT contained nickel, cobalt, iron, manganese and chromium. The AAS analysis showed that the contents of iron, chromium and nickel in MWCNT were 4,400, 48 and 17 ppm (wt/wt), respectively, and that the manganese and cobalt contents were below the quantitative detection limit of 6 ppm.

Discussion

Length and width of MWCNT fibers

The lengths and widths of MWCNT fibers measured in the present study are in good agreement with those reported by Takagi *et al*[1]. The fraction of fiber lengths exceeding 15 μm were apparently greater in the

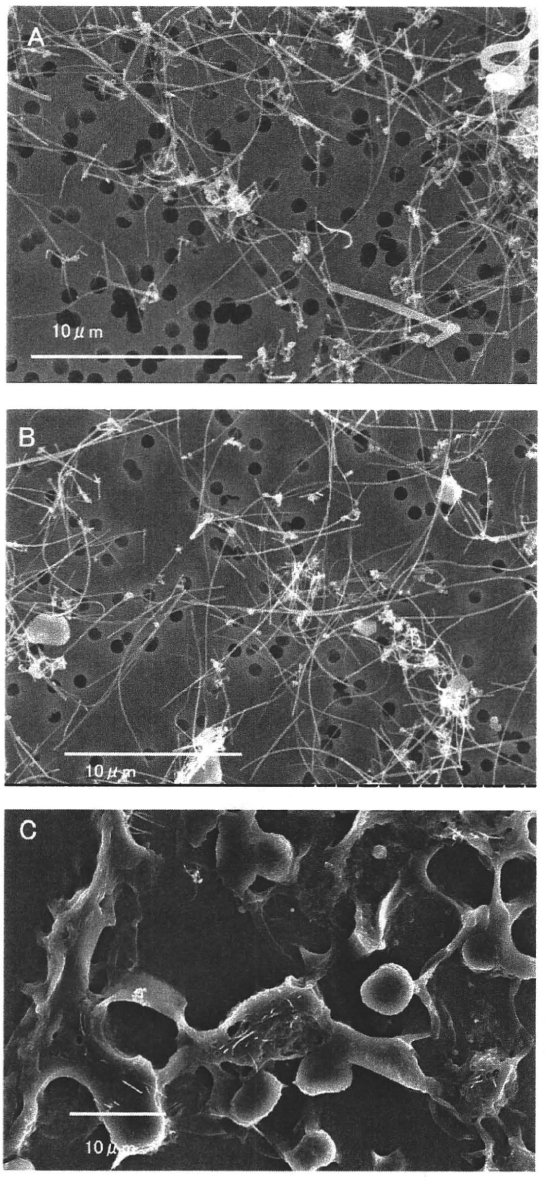

Fig. 5. SEM images of the MWCNT fibers, in the PBS-Tween 80 suspension, showing good dispersion of the fibers in the PBS-Tween 80 suspension after the 5-min ultrasonication (A), in the aerosolized MWCNT suspension ejected into air from the tip of the microspray cannula used for intratracheal instillation (B), and in the alveolar macrophages incompletely engulfing the well-dispersed MWCNT fibers in the alveoli of a rat lung on Day 1 after instillation of 160 μg MWCNT (C).
The concentration of MWCNT suspension used here was 533 μg/ml for samples A and B.

MWCNT used in the study of Poland *et al.*[3] than in the present study. Since we used the same MWCNT manufactured by Mitsui & Co. Ltd, there might be a difference in the measurement method of fiber length between the present study and that Poland *et al.*'study[3].

Indeed, we measured fibers greater than 0.5 μm in length on enlarged SEM photoprints. The present data of length and width of MWCNT fibers suggest that MWCNT might stimulate asbestos-like, length-dependent, pathogenic behavior in the lung. Poland *et al.*[3] demonstrated that long MWCNT fibers peritoneally injected in the abdominal cavity of female mice exert asbestos-like pathogenicity such as frustrated phagocytosis. Indeed, physical dimensions such as length and width of biopersistent fibers are known to be critically important determinants for the induction of mesotheliomas[15, 16]. Indeed, the length of asbestos fibers is known to be a critically important determinant for asbestos-induced carcinogenesis[14, 15]. *In vitro* exposure of cultured LLC-MK_2 cells to long crocidolite asbestos fibers was reported to induce formation of binucleated cells leading to polyploidy, resulting from sterical blocking of cytokinesis by long fibers[17]. Another key factor for pathogenic, asbestos-like behavior is whether MWCNT is persistent in the lung and pleural cavity in the same manner as in the case of asbestos fibers suggested by Donaldson and Tran[18]. Our separate paper[10] demonstrated that a single intratracheal instillation of well-dispersed MWCNT fibers in rats caused persistent deposition of MWCNT in the alveolar space and wall, in addition to a tendency of MWCNT deposition in the bronchus-associated lymphoid tissue to gradually increase after the instillation. Those results suggest that the MWCNT is persistent in the lung and pulmonary lymphatic vessels. Therefore, it can be inferred that different pulmonary toxicities might be manifested, depending on the length of MWCNT fibers and their biopersistence. A further study with long-term observation will be needed to examine the biopersistence of MWCNT in the lung and pleura.

Dispersion of MWCNT fibers in the suspension and in the lung tissue

Together with addition of Tween 80 into PBS, 5-min ultrasonication was found to facilitate good dispersion of the agglomerated MWCNT fibers in the suspension. Since Tween 80 was reported to increase the susceptibility to oxidative stress in rat thymocytes at 10–30 μg/ml under *in vitro* conditions[19], the concentration of Tween 80 used in the present study was fixed at a concentration of 0.1%, in order to keep good dispersion and to minimize the pulmonary toxic responses to Tween 80. In our intratracheal instillation study[10], MWCNT was suspended in the PBS containing 0.1% Tween 80 and ultrasonicated for 20 min with an ultrasonic homogenizer. Then, the ultrasonicated suspension of MWCNT was further subjected to additional ultrasonication for 30 s with a sonicator immediately before intratracheal instillation. This repeated ultrasonication was performed to maintain good dispersion of MWCNT in the suspension, because the MWCNT appeared visually to re-agglomerate when the suspension was left for about 30 min during the period for intratracheal instillation.

It is interesting to note in the present SEM observation (Fig. 5A) that some MWCNT fibers were overlapped and twisted with each other, but there were neither clumped nor aggregated particles. Besides, knot-like blocks at the ends of fibers were observed occasionally. Presumably, formation of the knot-like structure might be causally related to the presence of residual catalyst particles on which two or more filaments of MWCNTs grow during the gaseous CVD process. The simulation experiment (Fig. 1) revealed that the microspray cannula used in the present study would allow delivery of the MWCNT suspension as a mist-like colloid into the distal end of the trachea, as evidenced by the well-dispersed state of MWCNT fibers (Fig. 5B) similar to that seen in the suspension before the instillation. The SEM observation (Fig. 5C) evidenced that MWCNT fibers were well-dispersed in the alveoli on Day 1 after intratracheal instillation at a dose of 160 μg/rat. Notably, cytoplasmic penetration of the dispersed MWCNT fibers after phagocytosis by alveolar macrophages (Fig. 5C) could be categorized as frustrated and incomplete phagocytosis, as proposed by Poland *et al.*[3] and Hubbs *et al.*[20], respectively. Therefore, it can be concluded from both DLS measurement and SEM observation that the MWCNT fibers were well-dispersed in the suspension by 20-min ultrasonication in the presence of 0.1% Tween 80 as a dispersant.

Dispersion or agglomeration of SWCNT administered by intratracheal instillation and pharyngeal aspiration has been reported to affect the pulmonary toxic responses. Warheit *et al.*[6] reported that intratracheal instillation of SWCNT produced mortality due to suffocation in 15% of the dosed rats, resulting from mechanical blockage of the respiratory tract by SWCNT which was highly electrostatic and did not disperse into single fibers. Mercer *et al.*[5] reported that pharyngeal aspiration of well-dispersed SWCNT in mice induced a potent interstitial fibrotic reaction with wide distribution of the dispersed fibers into the alveolar interstitium in the absence of granuloma formation. On the other hand, Shvedova *et al.*[9] showed that pharyngeal aspiration of agglomerated, less-dispersed SWCNT in mice induced granulomatous lesions associated with hypertrophied epithelial cells surrounding SWCNT aggregate as well as inflammation and interstitial fibrosis. Taken together, it can be inferred that good dispersion of MWCNT fibers in the suspension and ultimately in the lung tissue might be involved in the rat pulmonary lesions induced by intra-

tracheal instillation of MWCNT pretreated in the same manner[10].

Metal impurities

MWCNT iron, chromium and nickel contents were 4,400, 48 and 17 ppm (wt/wt) in the present study. They were estimated to be equivalent to lung burden of 0.7, 0.0077 and 0.0027 μg/rat, respectively, when 160 μg of MWCNT were intratracheally instilled. We examined the pulmonary toxic responses to these metal impurities on the basis of a literature survey. Toya *et al.*[21, 22] reported that intratracheal instillation of chromium and nickel fumes in rats induced a slight degree of pulmonary lesions at doses of 3.4 mg Cr/kg and 1.4 mg Ni/kg body weight. It can be inferred on the basis of these reported findings that the administration of 0.0077 and 0.0027 μg/rat, which are equivalent to 0.031 and 0.011 μg/kg body weight, would not induce any pulmonary lesions. Shvedova *et al.*[7] reported that *in vitro* exposure of human keratinocyte cells to unrefined SWCNT containing 30% iron produced cellular toxicity and oxidative stress as detected by the electron spin resonance (ESR) of the iron. Kagan *et al.*[8] reported that iron-rich SWCNT (26% Fe) caused significant loss of intracellular low molecular thiols (GSH) and accumulation of lipid hydroxides in both zymosan- and PMA-stimulated RAW 264.7 macrophages as compared with iron-stripped SWCNT (0.23% Fe). Shvedova *et al.*[9] also showed that pharyngeal aspiration of the purified SWCNT containing 0.23% iron in mice at a dose of 40 μg/head (equivalent to 0.09 μg iron) did not generate detectable signals from iron paramagnetic centers readily detectable by ESR spectroscopy in the unrefined SWCNT. Assuming similar distribution of 0.7 μg iron in the present study and 0.09 μg iron in the study of Shvedova *et al.* over the alveolar epithelial surface area, and normalizing to the equivalent alveolar epithelial surface area in rats (0.392 m^2/lung) and mice (0.068 m^2/lung) from a published morphometric analysis[21], the amount of iron in the unit alveolar epithelial surface area would be 1.7 $\mu g/m^2$ for rats and 1.3 $\mu g/m^2$ for mice. Taking the results of the *in vitro* and *in vivo* studies by Shvedova *et al.* and Kagan *et al.*[7–9] into consideration, any pulmonary responses to 4,400 ppm iron in the MWCNT might not contribute significantly to the observed pulmonary responses to 160 μg MWCNT. It can be concluded that 4,400 ppm (wt/wt) iron, 48 ppm chromium and 17 ppm nickel in the MWCNT were below the levels that would elicit positive pulmonary toxic responses to these metals.

Conclusion

Length and width of MWCNT fibers, dispersion of MWCNT in the PBS suspension containing 0.1% Tween 80 after ultrasonication, and metal impurities of MWCNT were investigated for an intratracheal instillation study. Mean length and width of single MWCNT fibers as measured on SEM photographs were 5.0 μm and 88 nm, respectively, and the fibers longer than 5.0 μm were 38.9% of all fibers measured. Both DLS measurement and SEM observation revealed that the MWCNT was well-dispersed in the suspension, at the time of intratracheal instillation, and in the alveoli on Day 1 after instillation. The AAS analysis showed that MWCNT iron, chromium and nickel contents were 4,400, 48 and 17 ppm (wt/wt), respectively, all of which were below the levels that would elicit positive pulmonary toxic responses to these metals.

Acknowledgements

The present study was financially supported by a Grant-in-Aid for Scientific Research from the Ministry of Health, Labour and Welfare of Japan. The authors are deeply indebted to Dr. Haruhiko Sakurai, Professor Emeritus of Keio University, for his fruitful discussion in the present study and to Dr. Makoto Ohnishi of the JBRC for his excellent assistance with metal analysis in MWCNT.

References

1) Takagi A, Hirose A, Nishimura T, Fukumori N, Ogata A, Ohashi N, Kitajima S, Kanno J (2008) Induction of mesothelioma in p53+/– mouse by intraperitoneal application of multi-wall carbon nanotube. J Toxicol Sci **33**, 105–16.
2) Sakamoto Y, Nakae D, Fukumori N, Tayama K, Maekawa A, Imai K, Hirose A, Nishimura T, Ohashi N, Ogata A (2009) Induction of mesothelioma by a single intrascrotal administration of multi-wall carbon nanotube in intact male Fischer 344 rats. J Toxicol Sci **34**, 65–76.
3) Poland CA, Duffin R, Kinloch I, Maynard A, Wallace WAH, Seaton A, Stone V, Brown S, MacNee W, Donaldson K (2008) Carbon nanotubes introduced into the abdominal cavity of mice show asbestos-like pathogenicity in a pilot study. Nat Nanotechnol **3**, 423–8.
4) Driscoll KE, Costa DL, Hatch G, Henderson R, Oberdörster G, Salem H, Schlesinger RB (2000) Intratracheal instillation as an exposure technique for the evaluation of respiratory tract toxicity: uses and limitations. Toxicol Sci **55**, 24–35.
5) Mercer RR, Scabilloni J, Wang L, Kisin E, Murray

AR, Schwegler-Berry D, Shvedova AA, Castranova V (2008) Alteration of deposition pattern and pulmonary response as a result of improved dispersion of aspirated single-walled carbon nanotubes in a mouse model. Am J Physiol Lung Cell Mol Physiol **294**, L87–L97.

6) Warheit DB, Laurence BR, Reed KL, Roach DH, Reynolds GAM, Webb TR (2004) Comparative pulmonary toxicity assessment of single-wall carbon nanotubes in rats. Toxicol Sci **77**, 117–25.
7) Shvedova AA, Castranova V, Kisin ER, Schwegler-Berry D, Murray AR, Gandelsman VZ, Maynard A, Baron P (2003) Exposure to carbon nanotube material: assessment of nanotube cytotoxicity using human keratocyte cells. J Toxicol Environ Health A **66**, 1909–26.
8) Kagan VE, Tyurina YY, Tyurin VA, Konduru NV, Potapovich AI, Osipov AN, Kisin ER, Schwegler-Berry D, Mercer R, Castranova V, Shvedova AA (2006) Direct and indirect effects of single walled carbon nanotubes on RAW264.7 macrophages: role of iron. Toxicol Lett **165**, 88–100.
9) Shvedova AA, Kisin ER, Mercer R, Murray AR, Johnson VJ, Potapovich AI, Tyurina YY, Gorelik O, Arepalli S, Schwegler-Berry D, Hubbs AF, Antonini J, Evans DE, Ku BK, Ramsey D, Maynard A, Kagan VE, Castranova V, Baron P (2005) Unusual inflammatory and fibrogenic pulmonary responses to single-walled carbon nanotubes in mice. Am J Physiol Lung Cell Mol Physiol **289**, L698–L708.
10) Aiso S, Yamazaki K, Umeda Y, Asakura M, Takaya M, Toya T, Koda S, Nagano K, Arito H, Fukushima S (2010) Pulmonary toxicity of intratracheally instilled multi-wall carbon nanotubes in male Fischer 344 rats. Ind Health (in press).
11) Nano Carbon Thechnologies Co., LTD. The manufacturing process of MWCNT. http://www.nikkiso.co.jp/rd/main/014.html. (in Japanese) Accessed June 25, 2009.
12) Nikkiso Co., LTD. Development of arbon nanotube process in the nanotechnology world. http://www.nikkiso.co.jp/rd/main/014.html. (in Japanese) Accessed June 25, 2009.
13) Takaya M, Kohyama N, Serita F, Shinohara Y, Ono-Ogasawara M, Otaki N, Toya T, Takata A (2002). Analysis and biological effects of airborne rare-earth particles from functional materials. In: Kankyouhozen Kenkyuseikashu III. Japan Ministry of the Environment, Tokyo (in Japanese).
14) Morrow PE (1988) Possible mechanisms to explain dust overloading of the lungs. Fundam Appl Toxicol **10**, 369–84.
15) Pott F (1978) Some aspects on the dosimetry of the carcinogenic potency of asbestos and other fibrous dusts. Staub-Reinhalt Luft **38**, 486–90.
16) Stanton MF, Layard M, Togeris A, Miller E, May M, Morgan E, Smith A (1981) Relation of particle dimension to carcinogenicity in amphibole asbestos and other fibrous minerals. J Natl Cancer Inst **67**, 965–75.
17) Jensen CG, Jensen LCW, Rieder CL, Cole RW, Ault JG (1996) Long crocidolite asbestos fibers cause polyploidy by sterically blocking cytokinesis. Carcinogenesis **17**, 2013–21.
18) Donaldson K, Tran CL (2004) An introduction to the short-term toxicology of respirable industrial fibres. Mutat Res **553**, 5–9.
19) Tatsuishi T, Oyama Y, Iwase K, Yamaguchi J, Kobayashi M, Nishimura Y, Kanada A, Hirama S (2005) Polysorbate 80 increases the susceptibility to oxidative stress in rat thymocytes. Toxicology **207**, 7–14.
20) Hubbs A, Mercer RR, Coad JE, Barrelli LA, Willard PA, Sriram K, Wolfarth M, Castranova V, Porter D (2009) Persistent pulmonary inflammation, airway mucous metaplasia and migration of multiwalled carbon nanotubes from the lung after subchronic exposure. The Toxicologist (48th Annual Meeting of SOT) 457.
21) Toya T, Fukuda K, Kohyama N, Kyono H, Arito H (1999) Hexavalent chromium responsible for lung lesions induced by intratracheal instillation of chromium fumes in rats. Ind Health **37**, 36–46.
22) Toya T, Serita F, Sawatari K, Fukuda K (1997) Lung lesions induced by intratracheal instillation of nickel fumes and nickeloxide powder in rats. Ind Health **35**, 69–77.
23) Pinkerton KE, Gehr P, Crapo JD (1991) Architecture and cellular compositiom of the air-blood barrier. In: Treatise on pulmonary toxicology. Vol. 1. Comparative biology of the normal lung, Parent RA (Ed.), 121–8, CRC Press, Boca Raton.

Journal of Environmental Science and Health Part A (2010) **45**, 1616–1624

ISSN: 1093-4529 (Print); 1532-4117 (Online)
DOI: 10.1080/10934529.2010.506121

Taylor & Francis
Taylor & Francis Group

Chloroform distribution and accumulation by combined inhalation plus oral exposure routes in rats

MAKOTO TAKE[1], SEIGO YAMAMOTO[1], MAKOTO OHNISHI[1], MICHIHARU MATSUMOTO[1], KASUKE NAGANO[1], TAKASHI HIROTA[2] and SHOJI FUKUSHIMA[1]

[1]*Japan Bioassay Research Center, Japan Industrial Safety and Health Association, Hadano, Kanagawa, Japan*
[2]*Department of Biopharmaceutics, Faculty of Pharmaceutical Sciences, Tokyo University of Science, Noda, Chiba, Japan*

The present investigation was undertaken to determine the distribution and accumulation of chloroform in the blood, liver, kidney and abdominal fat of rats after simultaneous exposure by two routes, inhalation and oral. To distinguish the contribution of each route, unmodified chloroform ($CHCl_3$) was administered by inhalation and deuterated chloroform ($CDCl_3$) was administered orally. Exposure by inhalation and oral administration resulted in $CHCl_3$ and $CDCl_3$ concentrations in the tissues which were significantly higher than when exposure was by either inhalation or oral administration alone. This is the first study to follow the contribution of each of two routes of chloroform exposure on chloroform distribution and accumulation in target tissues. Our results indicate that when assessing the toxicity and carcinogenicity of chloroform, exposure routes, especially the effects of exposure by multiple routes, must be taken into consideration.

Keywords: Chloroform, deuterated chloroform, combined exposure routes, blood concentration, tissue concentration, mass spectrometer.

Introduction

Chloroform is widely used as an organic solvent during the synthesis of fluorocarbons, drugs and insecticide fumigants,[1] and substantial amounts have been released into the atmosphere and public water supply.[2,3] Chloroform is also produced by sanitary chlorination of drinking water. Andelman[4] and the Ministry of the Environmental Government of Japan[5] have reported that chloroform is present in outdoor and indoor air, community drinking water, and a variety of foodstuffs. Consequently, humans are potentially exposed to chloroform through various media including the air and water.

Chloroform is categorized as a possible human carcinogen (2B) by the International Agency for Research on Cancer (IARC).[1] Animal studies have shown that both inhalation[6] and oral[7,8] administration of chloroform induces kidney tumors in rats and mice. Importantly, a two year study using rats indicated that compared with either inhalation or oral administration alone, combined inhalation plus oral administration of chloroform markedly enhanced chloroform toxicity and tumor induction in the kidney.[9] This study concluded that the enhanced effect on renal toxicity and carcinogenicity of exposure to chloroform by inhalation plus oral administration was greater than additive. That the effect of exposure to a chemical mixture by multiple routes may be different from the additive effects of exposure by single routes is also espoused by the United States Environmental Protection Agency (US EPA).[10]

The blood concentration of chloroform,[11–15] the distribution of chloroform into the blood and tissues[16,17] and a physiologically based pharmacokinetic model for chloroform[18] after exposure by a single route have been described by previous papers. However, because of the non-additive effect of multiple-route exposure to chloroform, it is also important to determine the contribution of each route of a multiple-route exposure to the concentration of chloroform in the blood and tissues. The aim of the present study was to use 2 routes of exposure to chloroform, administration by inhalation and administration by oral gavage, and determine the contribution of each exposure route to chloroform concentrations in the blood and tissues. In order to assess each exposure route, we administered unmodified chloroform ($CHCl_3$) by inhalation and deuterated chloroform ($CDCl_3$) via oral gavage and analyzed $CHCl_3$ and $CDCl_3$ by mass spectrometer (MS). The present study is the first report on these determinations.

Address correspondence to Makoto Take, Japan Bioassay Research Center, Japan Industrial Safety and Health Association, Kanagawa, Japan; E-mail: m-take@jisha.or.jp
Received March 25, 2010.

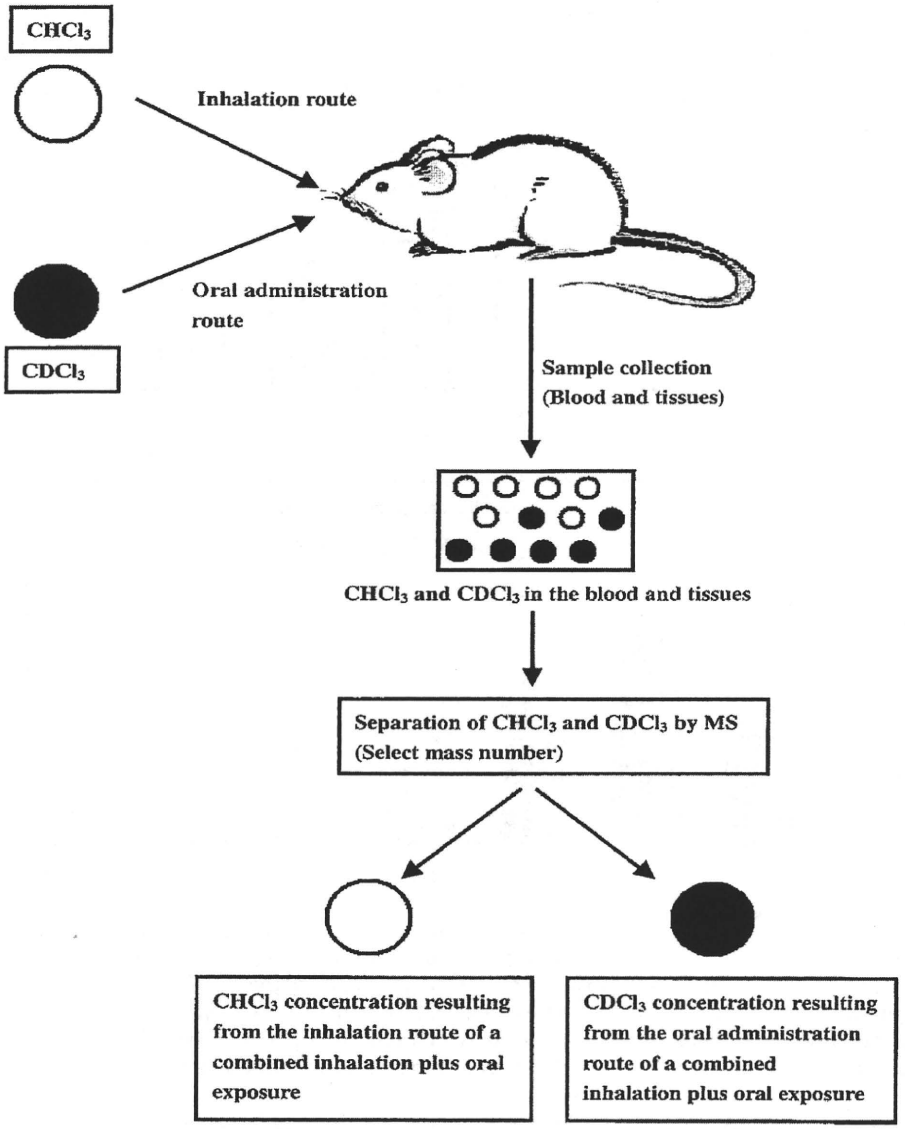

Fig. 1. Following the chloroform delivered by inhalation ($CHCl_3$) and the chloroform delivered orally ($CDCl_3$) when chloroform is administered simultaneously by inhalation and oral gavage.

Materials and methods

Chemicals

$CHCl_3$ (purity greater than 99.0%) used for inhalation administration was purchased from Wako Pure Chemical Industries, Ltd (Osaka, Japan) and $CDCl_3$ (purity greater than 98.0%) used for oral administration was purchased from Cambridge Isotope Laboratories, Inc (Andover, MA, USA).

Animal care

17-wk-old male F344/DuCrj SPF rats were purchased from Charles River Japan, Inc. (Kanagawa, Japan): body weights ranged from 243 to 301 g. Experiments were started after a one week acclimation period. The temperature and the relative humidity of the study were maintained in the ranges of 23 ± 2°C and 55 ± 15%, respectively. The animals were cared for according to the Guide for the Care and Use of Laboratory Animals,[19] and the present study was approved by the ethics committee of the Japan Bioassay Research Center (JBRC).

Study design

The rats were divided into 3 groups: inhalation administration, oral administration and combined inhalation plus oral administration. In the inhalation administration group, rats

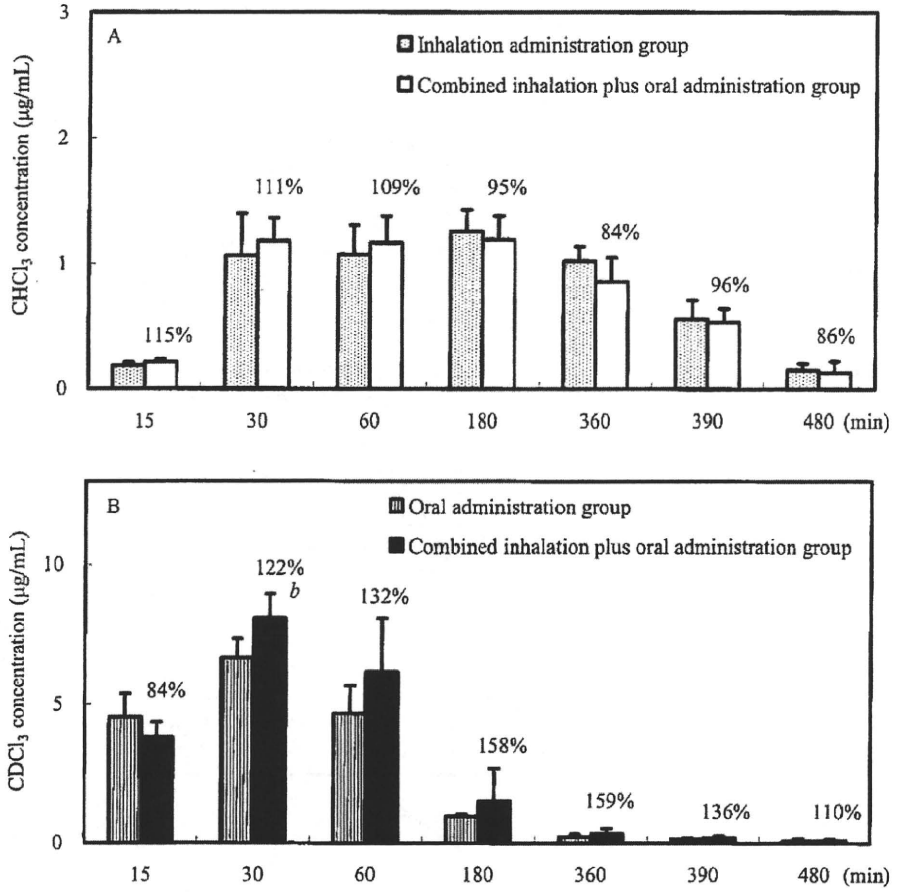

Fig. 2. $CHCl_3$ and $CDCl_3$ concentrations (mean ± SD) in the blood at each collection time point (n = 5 for each collection time/group): (A) Inhalation route. Numbers above the SD bars represent the percentage ratio of the $CHCl_3$ concentration in the blood of the combined inhalation plus oral administration group to the $CHCl_3$ concentration in the blood of the inhalation administration group at each collection time point. (B) Oral administration route. Numbers above the SD bars represent the percentage ratio of the $CDCl_3$ concentration in the blood of the combined inhalation plus oral administration group to the $CDCl_3$ concentration in the blood of the oral administration group at each collection time. [b]Significantly different from the oral administration group ($P \leq 0.05$).

were exposed to $CHCl_3$ by inhalation using whole-body inhalation chambers.[15] $CHCl_3$ vapor at a concentration of 100 ppm was generated by bubbling clean air through liquid $CHCl_3$. The $CHCl_3$ vapor concentration in the inhalation chambers was measured with gas chromatography (GC) using Agilent Technologies 6890 (Agilent Technologies, Santa Clara, CA, USA) every 15 min during the inhalation exposure period. The target concentration of $CHCl_3$ was 100 ppm (v/v) for 360 min. This dose is the same as one daily dose used by Nagano et al.[9] In the oral administration group, $CDCl_3$ dissolved in water (1000 ppm (w/w)) was orally administrated by stomach tube at a dose of 55 mg/kg body weight. This dose is equivalent to one daily dose of $CHCl_3$ administered at 1000 ppm $CHCl_3$ in the drinking water.[9] In the combined inhalation plus oral administration group, rats were exposed to $CHCl_3$ by inhalation at a target concentration of 100 ppm for 360 min immediately after the oral gavage of $CDCl_3$ at a dose of 55 mg/kg body weight (Fig. 1). The $CHCl_3$ vapor concentration in the inhalation chambers was 100.3 ± 0.99 and 100.4 ± 1.62 ppm (mean ± SD) in the inhalation administration and combined inhalation plus oral administration groups, respectively.

Blood and tissues collections and pretreatment for measurement

Forty-five rats in each group were used for examination of $CHCl_3$ and $CDCl_3$ concentrations in the blood and tissues. Blood was collected from the tail vein of each rat, and afterwards, necropsy was performed on the rats under ether anesthesia at 0, 15, 30, 60, 180, 360, 390, 480 or 1440 min after the start of inhalation administration or oral administration (5 rats were used for each collection time/group). The 0.2 mL blood samples were collected into 10-mL headspace sampler (HS)-vials and

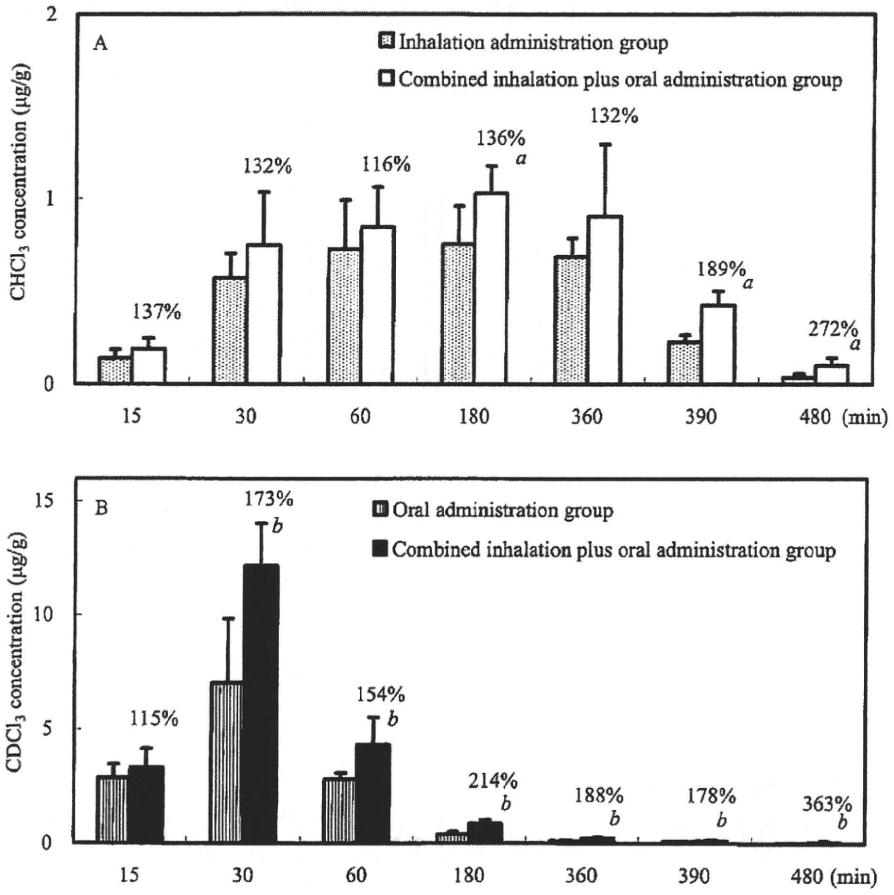

Fig. 3. $CHCl_3$ and $CDCl_3$ concentrations (mean ± SD) in the liver at each collection time point (n = 5 for each collection time/group): (A) Inhalation route. Numbers above the SD bars represent the percentage ratio of the $CHCl_3$ concentration in the liver of the combined inhalation plus oral administration group to the $CHCl_3$ concentration in the liver of the inhalation administration group at each collection time point. [a]Significantly different from the inhalation administration group ($P \leq 0.05$). (B) Oral administration route. Numbers above the SD bars represent the percentage ratio of the $CDCl_3$ concentration in the liver of the combined inhalation plus oral administration group to the $CDCl_3$ concentration in the liver of the oral administration group at each collection time. [b]Significantly different from the oral administration group ($P \leq 0.05$).

0.2 mL of distilled water was added to each sample. The liver, kidney and abdominal fat were removed from each rat and each tissue sample (liver, kidney and abdominal fat: range from about 0.1 to 1 g) was placed into a 10-mL HS-vial. 5 mL of distilled water was then added and the vials were immediately sealed with an aluminum crimp cup. $CHCl_3$ and $CDCl_3$ were not detected in the blood and tissues at time 0 or 1440 min (data not shown) in the 3 groups.

Measurement of $CHCl_3$ and $CDCl_3$ in the blood and tissues

The $CHCl_3$ and $CDCl_3$ concentrations in the blood and tissue samples were analyzed by HS-GC/MS using Agilent Technologies 7694 (Agilent Technologies) HS (oven temperature, 60°C; loop temperature, 80°C; vial equilibration time, 10 min (blood) and 30 min (tissues)) and Hitachi M-80B (Hitachi, Tokyo, Japan) GC/MS system (column, Agilent Technologies INNOWax 15 m × 0.53 mm i.d.; oven temperature, 80°C; ion source temperature, 250°C; carrier gas, helium at 10 mL/min; ionization, EI (electron ionization); collector slit, 150 μm; fragment peak, 82.946 m/z ($CHCl_3$) and 83.953 m/z ($CDCl_3$)).

Statistical analysis

Results are represented as means ± SD. Statistical comparison was performed between the single exposure route and the combined exposure routes using Student's *t*-test. A P value of 0.05 was considered significant.

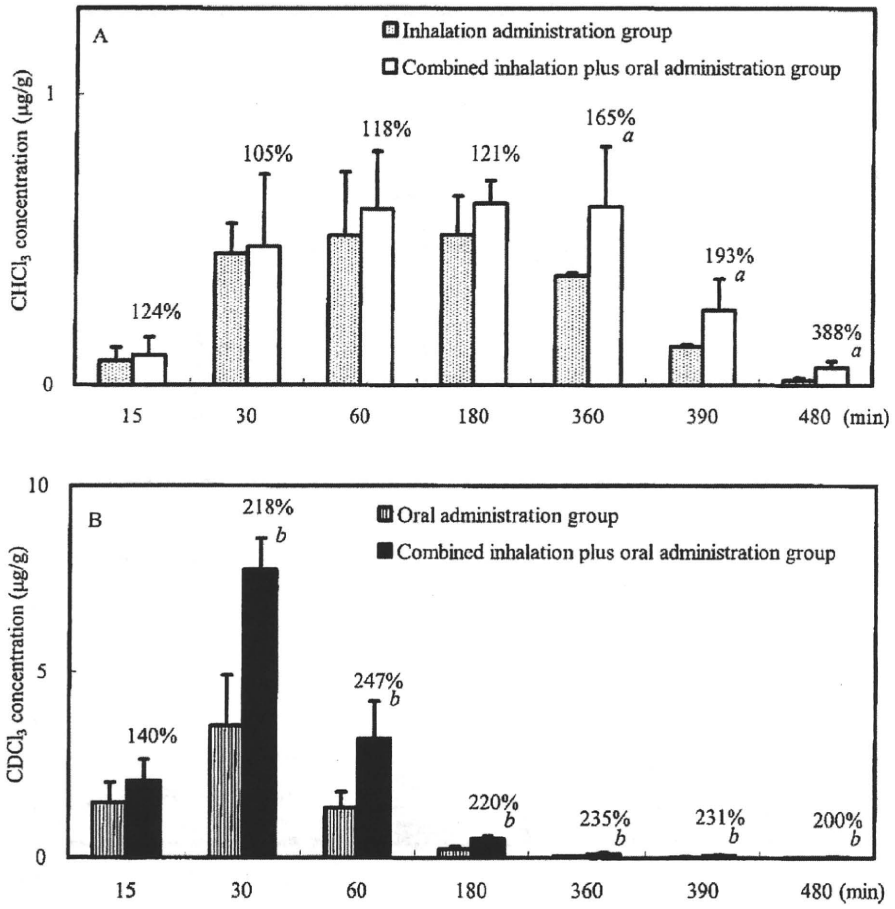

Fig. 4. $CHCl_3$ and $CDCl_3$ concentrations (mean ± SD) in the kidney at each collection time point (n=5 for each collection time/group): (A) Inhalation route. Numbers above the SD bars represent the percentage ratio of the $CHCl_3$ concentration in the kidney of the combined inhalation plus oral administration group to the $CHCl_3$ concentration in the kidney of the inhalation administration group at each collection time point. [a]Significantly different from the inhalation administration group ($P \leq 0.05$). (B) Oral administration route. Numbers above the SD bars represent the percentage ratio of the $CDCl_3$ concentration in the kidney of the combined inhalation plus oral administration group to the $CDCl_3$ concentration in the kidney of the oral administration group at each collection time. [b]Significantly different from the oral administration group ($P \leq 0.05$).

Results and discussion

Inhalation administration group

During the inhalation exposure period, $CHCl_3$ concentrations in the blood increased until 30 min after initiation of inhalation exposure and remained constant from 30 to 360 min (Fig. 2A). After the end of the exposure period, the $CHCl_3$ concentrations in the blood decreased over time. $CHCl_3$ remained detectable in the blood at 480 min (120 min after end of the exposure period). In this group the $CHCl_3$ concentration in the blood is governed by the blood-to-gas partition coefficient[20] and during the administration period the $CHCl_3$ concentration in the gas phase of the lung remained constant; therefore , the $CHCl_3$ concentration in the blood remained constant after equilibrium was reached. This pattern is very similar to the pattern of $CHCl_3$ concentration in the blood following inhalation of $CHCl_3$ vapor reported previously.[15]

The $CHCl_3$ concentrations in the liver and kidney also increased until 30 min and remained constant from 30 to 360 min (Figs. 3A and 4A). The $CHCl_3$ concentration in the liver and kidney of these rats is governed by tissue-to-blood partition coefficients[20] and elimination by metabolism[18,21–23] and excretion; the $CHCl_3$ concentration in these organs is expected to follow the observed pattern. In contrast, the $CHCl_3$ concentration in the abdominal fat increased throughout the exposure period (Fig. 5A). This is because $CHCl_3$ has high lipid solubility and the $CHCl_3$ concentration in the abdominal fat will increase until it reaches equilibrium with the blood as governed by the blood-fat partition coefficient.[18,24,25] After the end of the inhalation exposure period, the $CHCl_3$ concentrations

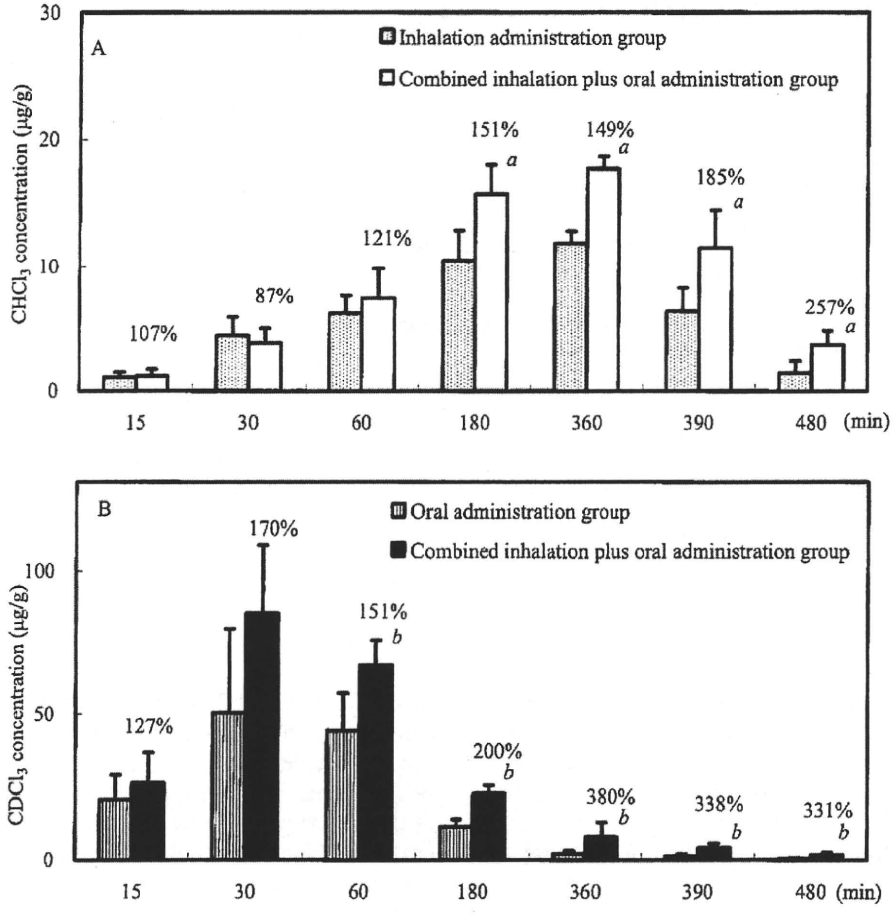

Fig. 5. $CHCl_3$ and $CDCl_3$ concentrations (mean ± SD) in the abdominal fat at each collection time point (n = 5 for each collection time/group): (A) Inhalation route. Numbers above the SD bars represent the percentage ratio of the $CHCl_3$ concentration in the abdominal fat of the combined inhalation plus oral administration group to the $CHCl_3$ concentration in the abdominal fat of the inhalation administration group at each collection time point. [a] Significantly different from the inhalation administration group ($P \leq 0.05$). (B) Oral administration route. Numbers above the SD bars represent the percentage ratio of the $CDCl_3$ concentration in the abdominal fat of the combined inhalation plus oral administration group to the $CDCl_3$ concentration in the abdominal fat of the oral administration group at each collection time. [b] Significantly different from the oral administration group ($P \leq 0.05$).

in all tissues decreased over time as $CHCl_3$ was eliminated from the body.

Oral administration group

The $CDCl_3$ concentration in the blood increased after administration, reaching a maximum concentration (Cmax) at 30 min and decreasing over time thereafter (Fig. 2B). $CDCl_3$ remained detectable in the blood at 480 min. Wang et al.[13] and Take et al.[26] reported time-course changes of $CHCl_3$ concentrations in blood following oral administration of $CHCl_3$ to rats, and the time-course changes of $CDCl_3$ concentration in the blood found in our study was very similar to their results. In addition, there are no differences in the chemical properties of $CDCl_3$ and $CHCl_3$, therefore, we conclude that $CDCl_3$ and $CHCl_3$ behave identically in our test animals.

The Cmax of $CDCl_3$ in the liver, kidney and abdominal fat was also reached at 30 min after oral administration and declined over time thereafter (Figs. 3B, 4B and 5B). $CDCl_3$ remained detectable in each tissue at 480 min. This pattern is due to the increase in $CDCl_3$ in the blood following oral administration of $CDCl_3$ and the elimination from the body of $CDCl_3$ over time. Since, the $CDCl_3$ concentrations in the tissues are dictated by the tissue-to-blood partition coefficients,[20] the general pattern of $CDCl_3$ concentration in the tissues is similar to that of the blood.

Combined inhalation plus oral administration group

The overall pattern of $CHCl_3$ concentration (inhalation route) in this group mirrored that of the single administration group. However, the $CHCl_3$ concentrations in the